Published paper

Brownjohn, J.M.W., Carden, E.P., Goddard, C.R., Oudin, G. (2010) *Real-time performance monitoring of tuned mass damper system for a 183 m reinforced concrete chimney*, Journal of Wind Engineering and Industrial Aerodynamics, 98 (3), pp. 169-179
http://dx.doi.org/10.1016/j.jweia.2009.10.013

Real-time performance monitoring of tuned mass damper system for a 183m reinforced concrete chimney

J.M.W. Brownjohn
Vibration Engineering Section, University of Sheffield, UK

E. P. Carden
Vibration Engineering Section, University of Sheffield, UK

R. C. Goddard
Bierrum International, UK

G. Oudin
Multitech, France

Contact author: Professor James MW Brownjohn
Department of Civil & Structural Engineering
University of Sheffield
Sir Frederick Mappin Building
Sheffield S1 3JD
E-mail: james.brownjohn@Sheffield.ac.uk
Tel: 0114-2225771
Fax: 0114-2225700

Abstract

A 183m reinforced concrete chimney for a coal-fired power station was instrumented in the latter part of its life during the construction of a replacement chimney. Because of concerns about large-amplitude response induced by interference effects from the new chimney in the prevailing upwind direction, a response monitoring system was installed, quickly followed by a tuned mass damper (TMD) system. As well as providing live display of the chimney response, the monitoring system was also used to check the functioning of the TMD. The monitoring system featured a direct implementation of the stochastic subspace identification procedure in the 'virtual instrument' controlling the system, so that modal damping values for the system were displayed automatically, in real time. The system thus provided an immediate visual indication of increased damping levels during strong winds, showing the correction functioning of the TMD. The paper describes the chimney, the monitoring system and its installation, the data processing and system identification procedure, together with performance data before, during and after installation of the TMD.

Keywords: Chimney concrete wind vortex shedding damping monitoring system identification

1 Introduction: large-amplitude oscillations and experimental studies of concrete chimneys

Performance of tall reinforced concrete chimneys due to both along-wind and cross-wind loading has long been a concern for operators of industrial facilities such as conventional power stations. Cross-wind effects are essentially dynamic, due to vortex shedding, and methods for calculating loading have been available for several decades (Maugh and Rumman, 1967).

Public domain information about poor in-wind performance of slender tall chimneys is rare, although catastrophic effects of wind-induced response were clearly demonstrated by the collapse of three cooling towers at Ferrybridge Power Station in 1965 (CEGB, 1965). Following this collapse the UK power generation utility began a program of research on performance of chimneys and cooling towers at their power stations (Armitt, 1969; Burrough, 1973; Burrough et al., 1972). A major factor at Ferrybridge was the interference effects of adjacent cooling towers, a problem that is also an issue for (tall) chimneys (Shears et al., 1980; Goddard, 2007; Vickery, 1980).

There have been several experimental studies of reinforced concrete chimneys which have naturally been related to concerns about wind-induced performance and primarily involved measurement of natural frequencies and damping ratios to be used in response predictions. One of the earliest techniques for recovering modal parameters (Scruton and Harding, 1957) used rocket thrusters to induce a significant initial deflection resulting in a transient decay dominated by the first vibration mode. From the decay trace the natural frequency and logarithmic decrement i.e. damping could be estimated with a high level of accuracy. Forced vibration has also been used, e.g. (Burrough et al., 1970) using a hydraulic ram attached to a suspended mass and driven by a white noise signal in order to evaluate the chimney performance at different levels of excitation. More recently (Da Rin, 1986) rotating eccentric mass shakers were used with the intention to engage significant levels of foundation motion so as to calibrate structural modeling of the entire structural system.

Such experimental campaigns with forced vibration involve considerable logistical difficulties so there are significant advantages with modern system identification procedures for civil structures that use only response data. ‘Operational modal analysis’ or OMA is a research growth area with a long history, and some of the early forms of OMA were used to recover modal parameters directly from the random response of chimneys due to normal wind excitation (Jeary, 1974) via autocorrelation functions.

Several more elaborate exercises (Sanada et al., 1992; Melbourne et al., 1983; Hansen, 1981; D'Asdia and Noe, 1998; Ruschewey and Galemann, 1996) have aimed at characterizing the nature of wind-induced response of chimneys by using pressure transducers and other instrumentation to record response signals. For the present study it is interesting to note that two of the these studies (Sanada et al., 1992; Melbourne et al., 1983) showed significant cross-wind response with the latter study successfully using pressure measurements to confirm that the cross-wind response was due to vortex shedding, but in none of these studies was there an opportunity to observe interference effects of upstream structures.

The research presented here originated when theoretical studies (Galsworthy and Vickery, 2006) predicted that excessive across wind oscillation of a 183m concrete chimney (Figure 1) might occur resulting from the up-wind construction of a replacement structure (Figure 2). The focus of this paper is the monitoring technology employed to track the performance of the chimney and evaluate the effectiveness of a tuned mass damper (TMD) that was installed to enhance the damping of the old structure and maintain its safety and serviceability during its remaining service life. By the time this paper is published the old chimney is likely to have been demolished.

The paper describes the chimney and the monitoring system designed initially to track performance of the unmodified structure and identify its dynamic characteristics. The TMD is briefly described, with a detailed description of significant modification of the monitoring system that enabled the functioning of the TMD to be tracked in real-time using an ‘output only’ OMA system identification procedure. The monitoring system was operational only briefly before the TMD was installed, hence all the interesting wind-induced response data are for the modified structure. Some of the most useful observations about the nature of the response and directional effects are reported here based on the first year of monitoring.

2 Rugeley stack and new chimney

The old chimney at the Rugeley Power Station, at coordinates 52 45'29.63"N 1 55'07.90"W, was constructed around 1968 and consisted of a 183m high reinforced concrete windshield, internally protected by a sectional, acid resisting brickwork lining supported from concrete corbels cast monolithically with the shell. The windshield tapered from an external diameter of 9.4m at the top to 15.7m at the base. Its outer surface suffered from the usual environmental actions and an external reinforced concrete cladding was installed in 1998 over the upper 24m. Figure 3 shows orthogonal elevations, showing the chimney as almost symmetric except for flue openings aligned with an axis between old and new chimneys.

Due to the installation of a flue gas desulphurisation plant, a new 183m chimney (Figure 2) was built in the vicinity of the existing chimney, at a distance of 110m and a bearing of 218°, approximately in the southwest direction of the prevailing winds in the UK. The two chimneys would coexist for approximately two years until demolition of the original chimney. Because of concern about interference effects due to the new chimney, a study of wind loads and interference effects (Galsworthy and Vickery, 2006) was conducted, which concluded that 'interference effects associated with the construction of the new chimney would significantly increase loads on the existing chimney'. The study indicated that maximum response of the existing chimney would occur with free-stream wind speed of 31m/sec and would depend strongly on the damping capacity.

The existing chimney was constructed at a time when high yield reinforcing steel was being introduced and laboratory testing of steel samples showed that mild steel reinforcing had been used. As a result, it was determined that the design capacity of the chimney would be exceeded over a substantial length at the critical wind speed for a damping ratio of 1% (Goddard, 2007).

Analysis of 17 years of wind data from the Pershore meteorological station gave a probability of 25% that the critical wind speed would be exceeded for directions within ±30° of the axis between the chimneys. Rather than strengthening or modifying the existing chimney for its remaining lifetime, it was decided first to install a response monitoring system capable of alerting operations staff at threshold response levels and later to install a tuned mass damper (TMD) to increase the chimney damping capacity and reduce interference-induced loads to below design capacity.

3 Monitoring system design

The monitoring system was deemed to be necessary to inform the power station operator about response levels and provide alarms depending on whether the chimney's dynamic displacement exceeded preset thresholds corresponding to critical stress levels. An optical system was ruled out for logistical and operational reasons, and since first mode response was expected to dominate in strong winds the displacement signals could be derived from acceleration signals.

Hence a simple acceleration monitoring system was designed comprising four accelerometers, arranged in biaxial pairs in watertight enclosures and a 4-channel National Instruments data acquisition (DAQ) system. The system specification was finalized by Bierrum on 16th January 2007 and it was installed on 2nd February. Honeywell QA750 quartz-flex servo-accelerometers were oriented in 'tangential' and 'radial' directions, with positive sensing axes aligned at compass bearings of 297° (radial) and 207° (tangential), locations determined by accessibility constraints. These axes differ by 11° from crosswind and alongwind axes with respect to wind coming from the direction of the new chimney.

The two accelerometer boxes (Figure 4) were installed by steeplejacks, who attached them to the exterior of the windshield at heights of 180m and 40m, with instrument cable tied at intervals to an existing power conduit for aviation warning lights. The purpose of measurements at the lower position was to provide a more accessible backup in case of problems with the accelerometers at the top level. With a reliable estimate of the operational deflection shapes around first mode frequency, top level response values could be estimated. Figure 5 shows the TMD under construction at a later date, with the lower accelerometer box visible at the level of the access rungs.

The system was initially left to run autonomously from 2nd February until the broadband internet connection line was installed. During this relatively short period signals from the top pair of accelerometers were lost and it was found that water under pressure from the signal cable was spraying into the instrument cabinet at the base of the chimney. The system was turned off until the problem could be fixed.

Concurrent with the early operation of the monitoring system, the power station operator began installation of a TMD system to control the chimney response. During the installation procedure, steeplejacks retrieved the upper accelerometer enclosure which was found to be dry inside with intact seals, and the cause of the water leak was identified as fraying of the instrument cable. The fraying was apparently caused by abrasion of the cable as it whipped against the wind shield concrete surface in strong winds, leading to abrasion and failure. Both instrument cables were replaced by significantly more rugged cables which were attached to the power conduit at shorter intervals (no more than one metre) and the system operated with only minor faults such as loss of ADSL connection and failure of power supplies to components of the DAQ system.

The monitoring system was originally designed to provide real-time measurements of the amplitude of movement of the stack and trigger alarm warnings when preset limits were breached. During high amplitude response the movement of the chimney was judged to be dominated by its fundamental mode response. Hence the trigger levels were converted from displacement values to acceleration values by simply multiplying by the squared first angular natural frequency.

4 Preliminary estimation of chimney dynamic characteristics

In addition to the amplitude measurements, estimates of the modal parameters were required to correlate with the structural model of the stack and for designing the TMD. Six minutes of data collected on 2nd Feb 2007 provided initial estimates for first bending mode frequency and damping values. The modal analysis of these very limited data (Brownjohn and Carden, 2007a) used both stochastic subspace identification (SSI) (Peeters and De Roeck, 1999) and eigensystem realization algorithm (ERA) (Juang and Pappa, 1985) applied to cross-covariance functions generated from the full six-minute record, decimated (with filtering) to a sample rate of 6.4Hz from the original 64Hz.

For the SSI procedure the first two modes were identified as 0.328Hz with 1.9% damping and 0.342Hz with 1.3% damping. Maximum order was 20 poles, since higher orders resulted in increasing numbers of apparently spurious poles. Using ERA and a fixed system order of 30, frequencies estimates of 0.326Hz and 0.342Hz agreed well but damping estimates converged at 0.8% and 0.2% as more lines of the covariance function were used (up to a maximum of 100). The second two bending modes were just below 1.4 Hz but their identification was not relevant for the monitoring application.

The initial estimates of natural frequencies were deemed to be reasonable but those of the damping were very suspicious, with no obvious reason for different damping values between the modes and the estimation procedures. The procedure described in (Reynders et al., 2008) was used with numerical simulation of an oscillator with frequency 0.31Hz and damping 1%, showing that expected standard deviation of damping for such an estimation using SSI would be at least 0.9%. The six minutes of data were simply too short to provide reliable damping estimates.

Unfortunately, due to the cable damage, further data were not available until 8th March. During a site visit to investigate the water ingress problem a little over two hours of data were recorded from the bottom set of accelerometers. Analysis of these data, described in detail elsewhere (Brownjohn and Carden, 2007a), showed that at least 20 minutes of response data were required for stable estimates of frequency (0.33Hz and 0.34Hz) with three times longer duration required for stable damping estimates of approximately 0.55% and 0.65%. Although variance errors are still high, these estimates are consistent with long-term averages of damping estimates obtained during subsequent operation in calm conditions i.e. with no functioning of the TMD, and provided a guide for data record length required for reliable estimation.

5 Remote monitoring operation

The installation of the broadband internet line was substantially delayed but on the 15th March remote monitoring was finally available and on 20th March, with access to the top of the chimney for TMD construction (Figure 5) the cabling for the top accelerometers was replaced so that signals could be obtained from all four accelerometers.

National Instruments SCC-AI13 low pass filter modules with cut off frequencies of 4 Hz were installed but unfortunately, being only 2-pole filters, a substantial amount of energy was being aliased making the first 4 Hz band very noisy. This was overcome by over-sampling at 64 Hz and digitally decimating the signal by a factor of eight (incorporating an eight pole Chebyshev filter). The data were collected in 180-second length frames and recorded on the local DAQ laptop computer. In addition the data were also transmitted over the broadband line using LabVIEW’s datasocket protocol for viewing at any computer equipped with the LabVIEW virtual instrument (VI) to read the data. The trigger levels were set centrally and also transmitted along with the data so that alarm conditions gave an audible and visual alarm.

The trigger levels for the top set of accelerometer responses consisted of three levels provided by Bierrum and related to displacement levels associated with the strength capacity of the concrete windshield. The highest response level represented 25cm with exceedence requiring site evacuation for personal safety. The bottom set of accelerometers was installed as a backup in case of failure of the top set and an outstanding issue was what values to set the trigger levels for the bottom set of responses to be consistent with those for the top set. This was resolved through analyzing data from 21st March to the 10th April from which it was possible to confirm the mode shape ordinate ratio. The estimates from data recorded when the RMS of the top accelerometers was below 0.005 were rejected as being too poor and the average mode shape ordinate ratio was estimated as 0.07, which as well as providing a fallback in the event of failure of the upper accelerometers also provided evidence of negligible foundation flexibility.

Consecutive three-minute data frames were transmitted by the DAQ laptop across the broadband internet connection and received by copies of a client application installed on multiple remote computers connected to the internet. The low sample rate of 8 Hz (after decimation) and low channel count resulted in relatively few data being transmitted compared to the capacity of the broadband line. The client application (Figure 6) displayed either the top set of accelerometer responses or the bottom set of responses depending on a toggle switch. The alarms were both visual and audible and triggered by either set of accelerometer responses exceeding the trigger levels set. The display and alarms were therefore based on the previous three minutes of data, considered to be close enough to real time for the power station's needs. A network connection alarm was also incorporated in case of a connection failure. One ongoing issue was that the datasocket connection became unstable approximately every three weeks and although the cause was not positively identified it was believed to be due to the opening and closing of many connections by the client applications at the sites of the various stakeholders. The only remedy to the problem was periodic system restarts during calm wind periods, taking only a few minutes. The system additionally saved and automatically emailed a log file of the daily summary statistics of the data collected, including the maximum and minimum values of the responses for each frame.

Figure 6 is the only recorded example of an alert condition due to large response levels and marks the strongest response levels recorded during the entire monitoring period. Although the trigger is based on peak response levels, the steep filtering (both analog and digital) has prevented noise spikes from generating false alarms and the more common alarm has been due to loss or degradation of internet connection at the client viewer.

6 Installation and operation of tuned mass damper (TMD), Figure 7

Multitech - France was awarded the order for the TMD on January 29th 2007. The time schedule was very important and the first steelwork was delivered to site on March 1st with the last items including the five viscous damping sets arriving on March 20th. The 42,000kg of moving mass plus the five viscous damper units were delivered within seven weeks of the order.

In order to limit the cost of erection the damper was designed so as to have the smallest moving mass possible consistent with being able to generate sufficient overall damping. It was also beneficial to limit the weight of the moving mass in order to simplify the connection of the brackets onto the old concrete shaft by using only post-drill anchors.

The design of the steel structure and moving mass had to be such as to allow all site adjustments without site welding as the shape of the stack would not be a perfect circle.

The design of the damper was done in order to allow as much as 450 mm relative displacement between the stack and the moving mass. The viscous dampers were tested in the laboratory in order to meet the design requirements and an extra length of pendulum was necessary to compensate for the stiffness of the viscous damping set which had also been determined in the laboratory.

Design assumptions for the TMD were for a damping coefficient of 18kNs/m and the pendulum was set for equivalent stiffness of 180kN/m. Based on a single chimney mode with frequency taken as 0.33Hz and for a modal mass of 1.28×10^{6}kg based on unit mode shape amplitude at the TMD level, the classical solution for the resulting two degree of freedom system would be a pair of modes with 0.306Hz and 0.356Hz having respective damping ratios of 4.6% and 6.7%. For reference, the chimney frequency would drop very slightly to approximately 0.325Hz were the TMD mass connected rigidly.

Verification of the performance of the TMD via site measurement, described in the next section, showed that the reality was rather different but that the TMD provided for up to 4% damping for the strongest motion and that it was effective in limiting chimney response to safe levels throughout its operational life.

7 Verification of the TMD

Following the installation of the tuned mass damper, Bierrum needed to check its continued correct operation and impact on the structural response. Hence it was decided to extract the damping parameters of the first two bending modes automatically online. From a previous implementation at the Tamar suspension bridge (Brownjohn and Carden, 2007b) the first two authors had experience in batch processing large amounts of data to extract modal parameters using Stochastic Subspace Identification (SSI) and this method was chosen due its numerical robustness and lack of need for user interaction. Reference based covariance-driven SSI (Peeters and De Roeck, 1999) was implemented using the Mathscript language of LabVIEW.

Due to the requirement for real-time identification, speed of computation was a very important issue. Data-driven SSI requires a QR decomposition of the Hankel matrix of the responses. The formation of a Toeplitz matrix of the covariances of the responses is the equivalent step in covariance-driven SSI and this is computationally quicker, and for this reason it was preferred. At the time of the original implementation the linear algebra functions of the Mathscript language were not as fast as those of MATLAB-based procedure used in the Tamar system and this meant that processing of each three minute frame within three minutes was not possible, considering the computer overhead processing other tasks associated with the DAQ and monitoring. The processing of three minute frames was not desirable in any case as the identification of damping from six minutes of data has already been described as having had too large a variance to be practically useful. As a result, and guided by the experience with the larger (two hour) dataset, a second VI was written which operated in tandem with the acquisition VI on a timed two hour loop.

The SSI VI loaded the previous two hours of data recorded on the DAQ laptop and identified the modal parameters of the first two bending modes. The data were first additionally decimated by four using an eight pole Chebyshev filter giving a new sampling frequency of 2 Hz then fed to the Mathscript functions to identify the modal parameters. Covariance-driven SSI requires several user input parameters such as maximum system order and number of lags (samples) of the covariance functions, and the selection of the values for these parameters was based on analysis of the previous data collected from the chimney. The top two accelerometers were used as the reference sensors since the resulting stability diagrams were cleaner than using all four channels as references. Twenty lags (instances) of the covariance functions were chosen to build the Toeplitz matrix which was decomposed once using singular value decomposition. The system matrices were then constructed with orders of 1 to 20. Given that both first modes were excited the majority of time, a minimum order of 4 was required before any reasonable identification was found. When analyzing just one frame of data a stability diagram is commonly constructed and examined to identify the poles which represent real modes of the structure. A typical stability diagram formed with the above settings is shown in Figure 8, with the power spectrum of the four accelerometers underlaid. The criteria used to define a pole as stable were that when compared with a pole from the previously identified model order, the frequency had to be within 1 %, the damping had to be within 5 % and the modal assurance criterion (MAC) value had to be within 2 %. Of course, in automatic modal analysis a stability diagram is not formed for the analyst to examine; to replace this step, in this and other implementations, a mode is extracted when a set of more than five stable poles is formed in a column. The modal parameters in this case were taken as the average values of those stable poles. The first two modes are clearly identified in Figure 8 with 15 stable poles for the first mode and 13 for the second mode. The third stable set of poles at about 0.8 Hz are a result of the signal processing applied to the signal (the Chebyshev filter applied during decimation) and were easily discarded as not representing a real physical pole as well as having unrealistic damping. This choice of parameters was found to work very well in practice.

The client monitoring software graphically displayed the previous few days of estimated damping parameters. This long term trend was required to monitor the performance of the TMD whose operation proved to be amplitude dependent, as expected. The TMD was not apparently engaged substantially during periods of weak wind and the damping parameters were identified with a higher variance when the modes were weakly excited. No trigger levels were set for the damping parameters but rather the trend in the parameters was eyeballed. This is acceptable because the TMD was not expected to have any sudden failure but rather a slower deterioration due to say water ingress to the damping fluid baths, giving due warning for maintenance. A log file of daily estimates of the modal parameters of the first two modes was also saved and emailed each day by the system.

Figure 9 is a screenshot of the damping plot for June 2007 showing a number of features. The damping values appear to have been stable below 1% up to 25th June when the values rose progressively to around 3% due to strong winds (associated with the heavy downpours that led to flooding throughout the UK in 2007). Around 22nd June and at the end of the data sequence, zero values are indicated, showing that no mode met the criteria for a stable identified mode. Likewise some outlying values are present. Small adjustments were subsequently made to the system (during operation) including rejection of modes higher than 0.5Hz, so cleaner damping data were produced.

The SSI procedure identified the modal parameters of the system comprising the TMD and the chimney, which for the classical case would replace the original two modes with four. No such mode splitting was ever observed (over the entire monitoring period) for the same number of poles (order) in the stability plot. Increasing the order of the identification process did however encourage it to find ever increasing numbers of extra modes centred on the original pair, but these all showed the signs of being mathematical artifices, rather than genuine structural modes.

Another logical question about the performance of the identification procedure would be about the effect of nonstationary response during the two hours of response used for each estimate. Certainly the TMD damping rate varied during the two-hour period used for each estimation, but there is no identification procedure that could be used in such an application to handle such a non-stationary system. However, assuming the range of responses to keep the TMD operational and provide stable damping levels, then SSI is robust to non-stationary excitation and the estimates are valid (Benveniste and Mevel, 2005).

8 Characteristics of response during and after installation of TMD

Because of the loss of signals from the upper accelerometer box until the TMD was installed, there are no useable data describing the wind-induced response of the bare unmodified chimney. The TMD installation was completed on 5th Apri 2007 and modal analysis of downloaded signals recorded from March 21st to April 20th is presented in Figure 10. This shows that for the majority of the time, damping levels were below 1%, until about a quiet week after the TMD installation was completed when damping levels began to increase noticeably. Modal frequency variation appears to show a changed pattern, but the reliability of the estimates is reduced due to the calm conditions.

Data available since the TMD installation include time series of response continuously recorded, with short breaks during system resets, emailed daily summary files of maxima and minima for each channel during each three-minute frame and daily summaries of frequency and damping values for two-hour frames. Also limited wind data were obtained from an anemometer on site and one-hour average values were obtained via http://weather.noaa.gov/ for the weather station at Birmingham Airport (EGBB: 52°27'13.47"N 1°43'55.56"W), at a distance of 37km, and East Midlands Airport (EGNX: 52°49'36.08"N 1°19'42.95"W) at a similar distance of 40km, to the east.

Some attempts were made to correlate damping estimates and frequencies with response levels and wind conditions, with no significant result. Weather data have thus been used as general indicators of prevailing conditions.

Figure 11 shows a collection of examples of acceleration signals rotated to northings and eastings, at the stated date/time. The diagonal straight line shows the cross-wind direction for winds coming from the direction of the new chimney. A relevant question is whether interference effects are visible in the observed performance. The wind engineering study (Galsworthy and Vickery, 2006) suggests that such effects should have occurred for winds with bearings in line with the new chimney, plus or minus a generous margin, and that with 5% damping, peak tip displacement would be approximately 120mm at the critical wind speed of 30m/sec. The largest recorded response, which occurred on 31st January 2008 is illustrated in Figures 6 and 11a and matches this value, with average winds up to 40mph (17.8m/sec, logged at EGBB) from SSW direction, which would include gusts around the critical speed. Figure 11b shows highly aligned response due to strong north-westerly winds.

Figures 11c and d show response due to lighter winds, Figure 11c representing decay due following a presumed strong gust, degenerating from a strongly aligned motion to the type of low-level response of Figure 11d. Figure 11e shows response due to the strongest south easterly winds observed during the monitoring. Wind speeds on March 12th approached the same levels as those on 31st January but were closer to the westerly direction and peak response levels (Figure 11f) were no more than one third the 31st January values. Similarly strong winds were not observed from NNE direction during the monitoring period, and for lower wind speeds the response levels (e.g. Figure 11g) showed cross-wind response picking up at similar wind speeds observed to trigger a dominant crosswind response for other wind directions. These figures suggest the conclusion that the mechanism is vortex shedding but that for the critical direction response is enhanced.

Finally Figure 11h shows response during UK's strongest earthquake in 20 years, in the early hours of 27th February, during which time it was also rather windy. This event appears to have had energy focused in frequency range 1 to 6Hz, exciting the higher chimney modes far more strongly than wind at any time.

Figure 12 (upper) shows the variation of peak responses for 3-minute frames and damping and frequency estimates for the first of the two fundamental modes for 2-hour frames during the monitoring up to mid-March 2008. Clearly radial response dominated, not least because that was the cross-wind alignment for prevailing strong winds.

9 Online damping and frequency estimation

The damping values obtained during remote automated operation and shown in Figure 12 suggest lower bounds for zero response at around 0.5%, rising to over 4% during periods of strong response. This range reflects a form of nonlinearity that would be a challenge to characterise reliably by observation of wind-induced response alone. A reliable identification using forced vibration or step relaxation was neither feasible nor necessary, but checks on extended high-amplitude directionally aligned response (downloaded for 29th February 2008) were made using the random decrement procedure (Cole, 1973). These showed damping estimates ranging from 3.3% in the direction of the weaker response and trigger threshold 0.017m/sec^2 (80% of RMS value for the six-hour period studied) with 3.9% in the stronger direction for 0.05m/sec^2 trigger, rising to 4.3% for 0.1m/sec^2 trigger threshold.

Via numerical simulations (Reynders et al., 2008) the expected (lower bound) standard deviation for SSI estimates of frequency and damping using the two-hour data sets are 0.0005 Hz and 0.19%. The damping values in both Figures 10 and 12 when the TMD is not engaged could therefore be expected to vary by at least +/- 0.2 % simply because of the limitations of the system identification algorithm employed. The plausibly non-Gaussian and certainly non-stationary nature of the excitation in reality, together with the smearing of all contributions to the damping (e.g. non-linearity of the TMD and aerodynamic effects) into a single value of equivalent viscous damping meant the estimated damping value would have a larger variance in practice. The relatively large scatter in the damping estimates compared to the natural frequency estimates in the figures is therefore explicable and enforced the applied philosophy of judging the performance of the TMD over many identifications of damping (the underlying trend) rather than a single identification, which was embodied in the monitoring panel of Figure 9.

The frequency estimates illustrated in Figure 12 are particularly interesting although they show no apparent relationship with the other response parameters, other than a diurnal variation. There are occasional significant drops in frequency that do not correspond with unusual weather conditions and the only possible explanation is likely to be changing operational conditions in the power station. Data corresponding to sub-zero temperatures show slightly higher values compared to periods in the summer, but the variations are small in comparison to the previously noted marked frequency drops. While Figure 12 gives the impression of scatter in the frequency estimates, zooming in the time axis shows clear diurnal variations evident in Figure 10.

Because the SSI procedure does not guarantee to identify both fundamental modes it is not a simple procedure to separate them out from the collective results, and Figure 12 shows only the lowest frequency mode identified. Figure 13 shows the distribution of all first mode frequency and damping ratios until March 2008; the bimodal distribution of frequencies has peaks around 0.328Hz and 0.336Hz with no values exceeding 0.34Hz, the lowest value recorded for the second of the two modes before the TMD began functioning. The damping distribution shows a single mode at 0.7% which coincides with the preliminary estimate of chimney damping without a functioning TMD.

In Figure 10, which shows the two fundamental modes during the time the TMD began operation, as well as the expected diurnal effect, the separation of fundamental mode frequencies in the two directions also varies, but with no identifiable correlation with the only available measure of response. These frequencies variations, whatever their origin, have implications for TMD design, requiring ability to operate over a wide range of structure mode frequencies.

10 Conclusions

This study was initiated by predicted excessive across-wind response of the existing chimney arising from its replacement being constructed in the prevailing upwind direction. As a result a performance monitoring system was installed and a tuned mass damper (TMD), believed to be the largest of its type, was constructed to improve the damping characteristics of the old chimney. Both the TMD and the monitoring system worked well; soon after the monitoring system was commissioned, the TMD was completed and the monitoring system was upgraded to track the chimney damping.

The damping values, which were reported effectively in real time, show the TMD to have been effective in controlling response. This response, in which cross-wind motion dominated in strong winds, appeared to fit predictions of interference effects. However one year of monitoring data is probably too little to provide conclusive proof, and wind data for the site are not adequate to assist.

Despite the short duration of the monitoring and lack of reliable on-site wind data, there are useful results in relation to damping and frequency values and implications for design of TMDs, the nature of performance at low and high wind speeds, and interference effects due to upstream structures.

11 Reference List

Armitt, J., 1969. Wind-excited vibration of chimneys. Central Electricity Research Laboratories, RD/L/N 89/69, Leatherhead, Surrey

Benveniste, A., Mevel, L., 2005. Nonstationary consistency of covariance based subspace methods. In: 44th IEEE Conference on Decision and Control, and the European Control Conference 2005, Seville, 7096-7101

Brownjohn, J. M. W., Carden, E. P., 2007a. Reliability of frequency and damping estimates from free vibration response. In: The 3rd International Operational Modal AnaIysis Conference, Copenhagen, Denmark,

Brownjohn, J. M. W., Carden, E. P., 2007b. Tracking the effects of changing environmental conditions on the modal parameters of Tamar Bridge. In: 3rd International Conference on Structural Health Monitoring and Intelligent Infrastructure, Vancouver, Canada,

Burrough, H. L., 1973. Dynamic characteristics of the Fawley chimney. Central Electricity Research Laboratories, RD/L/N 5/73, Leatherhead, Surrey

Burrough, H. L., Jeary, A. P., and Wilson, J. M., 1972. Vibration measurements on the Drax gas turbine chimney. Central Electricity Research Labs, RD/L/N 167/72, Leatherhead, Surrey

Burrough, H. L., Kinloch, H., Winney, P. E., 1970. Vibration studies on full-scale stuctures. In: Dynamic Waves in Civil Engineering, UC Wales, 445-472

CEGB, 1965. Report of the committee of inquiry into the collapse of cooling towers at Ferrybridge on November 7, 1965. Central Electricity Generating Board,

Cole, H. A., 1973. On-line failure detection and damping measurements of aerospace structures by random decrement signatures. NASA CR2205,

D'Asdia, P., Noe, S., 1998. Vortex induced vibration of reinforced concrete chimneys: in situ experimentation and numerical previsions. Journal of Wind Engineering and Industrial Aerodynamics 74-76, 765-776.

Da Rin, E. M., 1986. Dynamic structural testing of Torre Valdaliga Nord power plant 250m high multi-flue chimney. In: XXV CICIND Meeting,

Galsworthy, J. K. and Vickery, B. J., 2006. Wind loads and interference effects for new and existing chimneys at the Rugeley power station, UK. Alan Davenport Wind Engineering Group, Boundary Layer Wind Tunnel Laboratory, London, Ontario, Canada, N6A 5BP

Goddard, C. R., 2007. The design of the 183m new chimney, Rugeley, UK -interference effects. In: CICIND, Esbjerg, Denmark,

Hansen, S. O., 1981. Cross-wind vibrations of a 130-m tapered concrete chimney. Journal of Wind Engineering and Industrial Aerodynamics 8, 145-155.

Jeary, A. P., 1974. Damping measurements from the dynamic behaviour of several large multi-flue chimneys. Proceedings of the Institution of Civil Engineers 57, 321-329.

Juang, J.-N., Pappa, R. S., 1985. An eigensystem realization algorithm for modal parameter identification and model reduction. Journal of Guidance 8, No. 5**,** 620-627.

Maugh, L. C., Rumman, W. S., 1967. Dynamic design of reinforced concrete chimneys. ACI Journal 64-47, 558-567.

Melbourne, W. H., Cheung, J. C. K., Goddard, C. R., 1983. Response to wind action of 265m Mount Isa stack. ASCE Journal of Structural Engineering Vol. 109, No. 11**,** 2561-2577.

Peeters, P., De Roeck, G., 1999. Reference-Based Stochastic Subspace Identification For Output-Only Modal Analysis. Mechanical System & Signal Processing 13, No. 6**,** 855-878.

Reynders, E., Pintelon, R., De Roeck, G., 2008. Uncertainty bounds on modal parameters obtained from stochastic subspace identification. Mechanical Systems and Signal Processing 22, No. 4**,** 948-969.

Ruschewey, H., Galemann, T., 1996. Full-scale measurements of wind-induced oscillations of chimneys. Journal of Wind Engineering and Industrial Aerodynamics 65, No. 1-3**,** 55-62.

Sanada, S., Suzuki, M., Matsumoto, H., 1992. Full scale measurements of wind force acting on a 200m concrete chimney, and the chimney's response. Journal of Wind Engineering and Industrial Aerodynamics 41-44, 2165-2176.

Scruton, C. and Harding, D. A., 1957. Measurement of the structural damping of a reinforced concrete chimney stack at Ferrybridge 'B' power station. NPL Aero Report NPL/Aero/323,

Shears, M., Reynolds, Saxon, A. E., Levy, J., 1980. Informal discussion. Wind dynamics of chimneys and masts. Proceedings of the Institution of Civil Engineers, Part 1 68, No. 2.

Vickery, B. J., 1980. Across-wind buffeting in a group of four-in-line chimneys. In: Proceedings, 4th Colloquium on Industrial Aerodynamics, Aachen, 169-182

12 Figures

Figure 1 Chimney at Rugeley Power station

Figure 2 New Chimney under construction

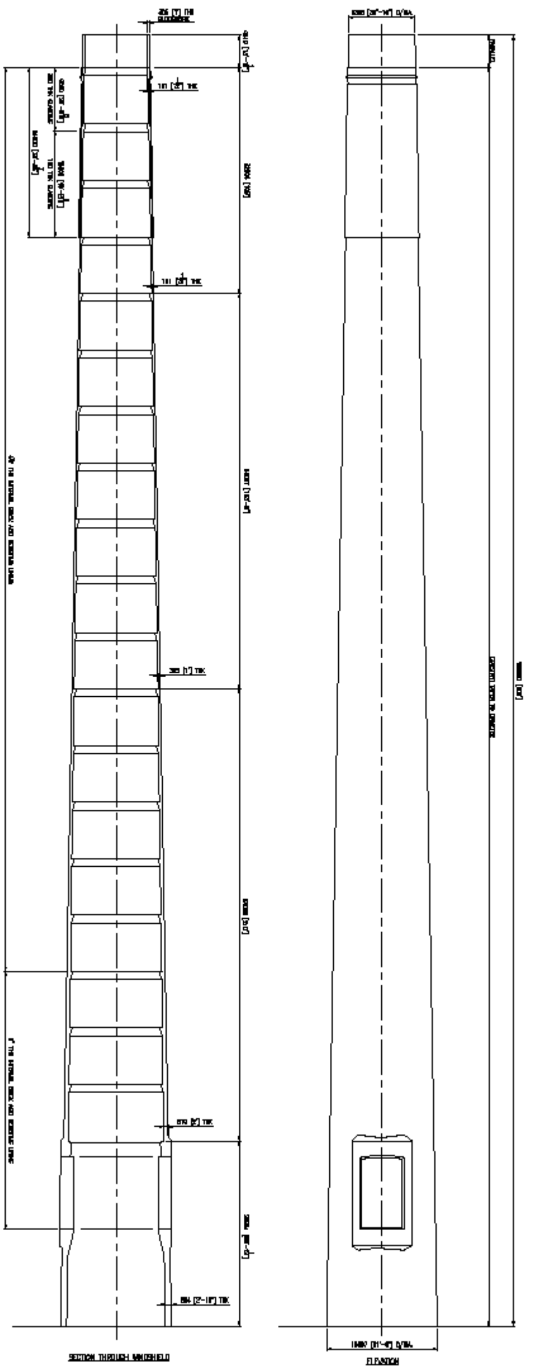

Figure 3 Orthogonal elevations of Rugeley Chimney, with external diameters 15.7 m and 9.4 m at base and tip respectively

Figure 4 Accelerometer boxes, with curved and slotted plates for easy attachment

Figure 5 TMD under construction, with lower accelerometer box in position and flue openings flanking chimney

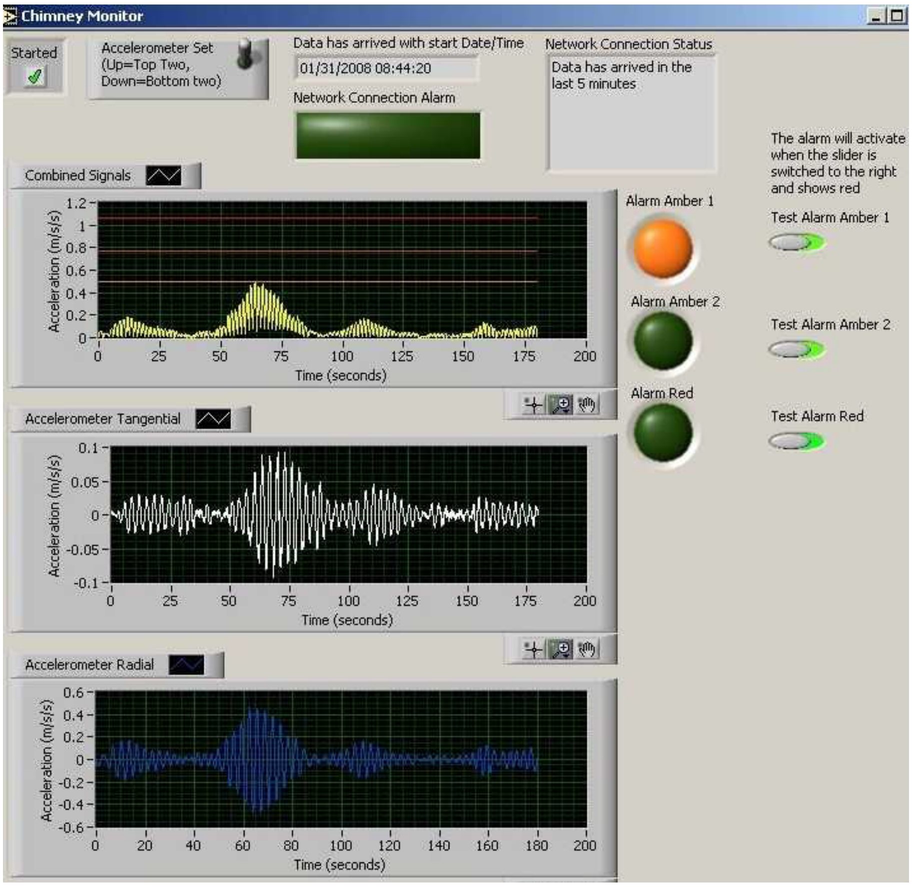

Figure 6 Monitoring system indicating alert level Amber 1, 31/01/2008

Figure 7 View from new chimney showing TMD supports, mass ring and dampers

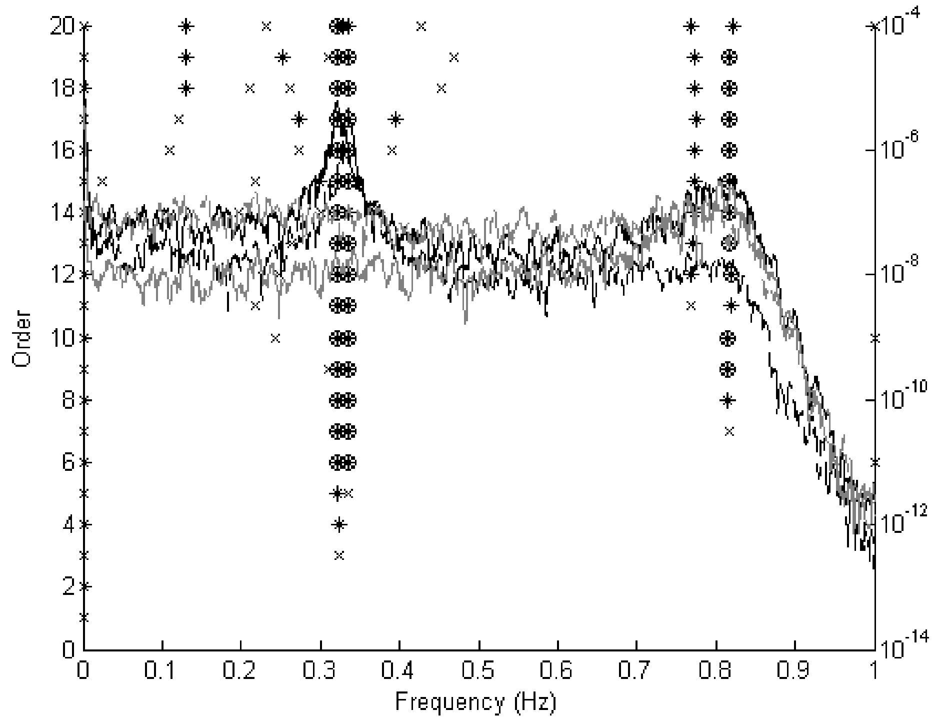

Figure 8 Typical stability diagram obtained from decimated response data. 'x' are non-stable poles, stars are stable in frequency only, circles are stable poles. Black solid and dashed lines are power spectrum of top two accelerometers, grey solid and dashed lines are power spectrum of bottom two accelerometers

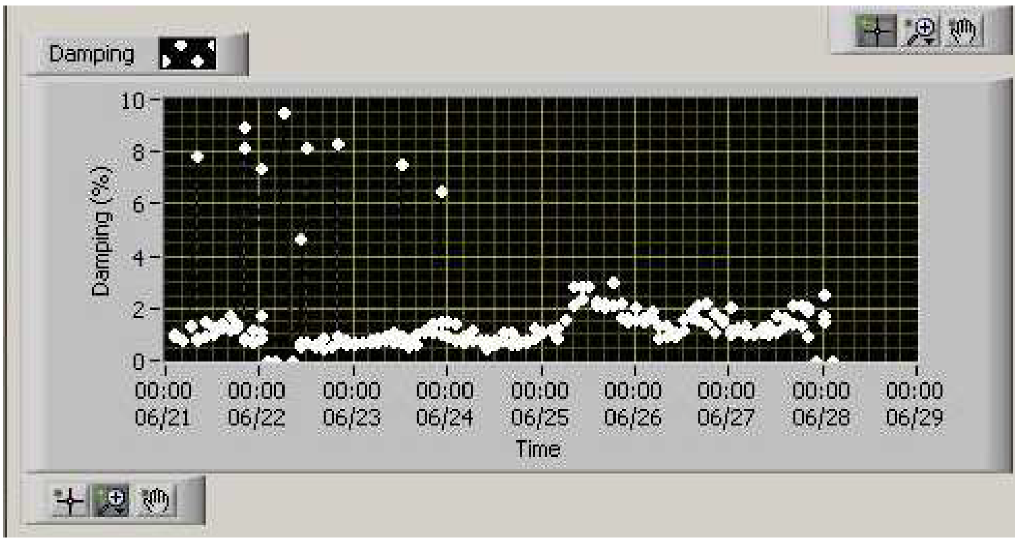

Figure 9 Damping values from seven days of monitoring, varying from 0.5% to 3%

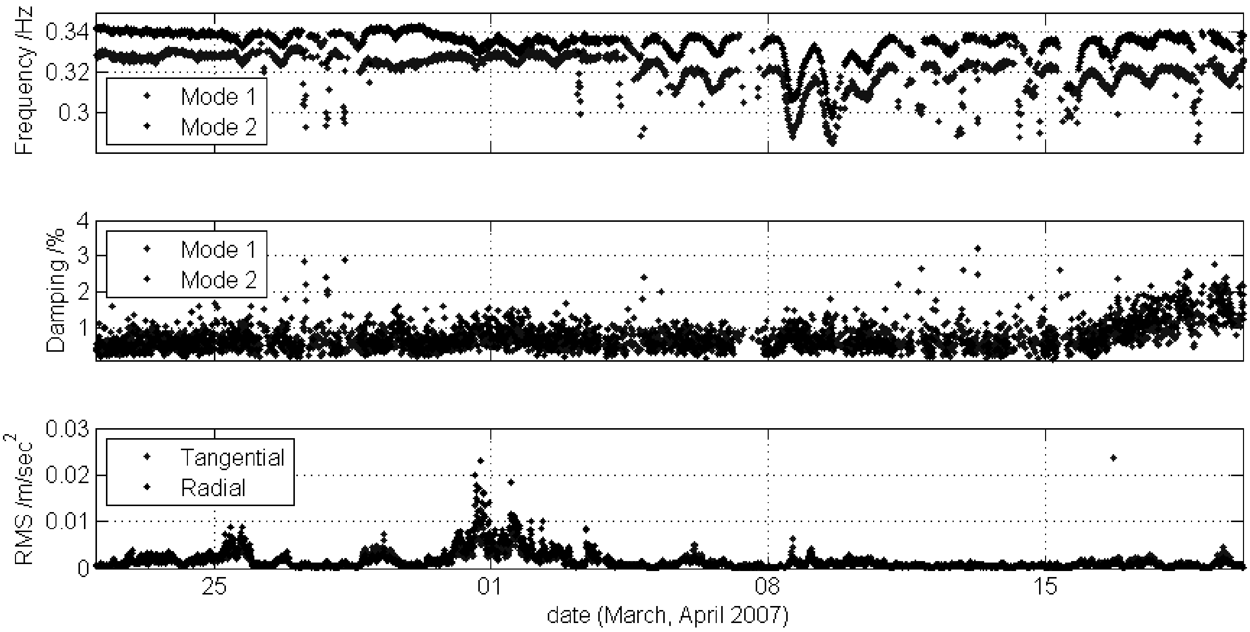

Figure 10 Variation of fundamental mode frequency and damping and of chimney response levels over 18-minute frames during 31 days of operation spanning commissioning of the TMD

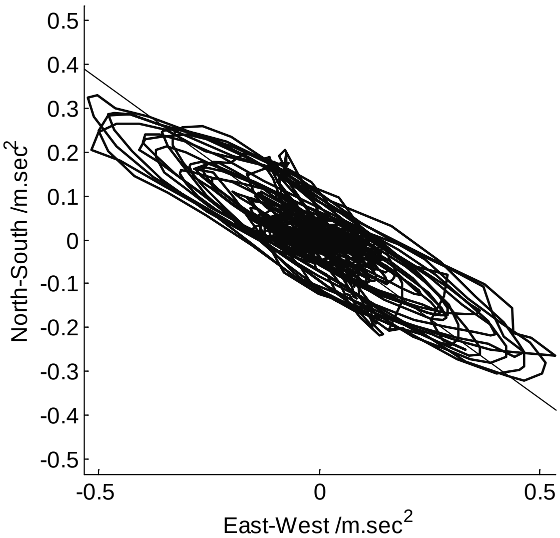

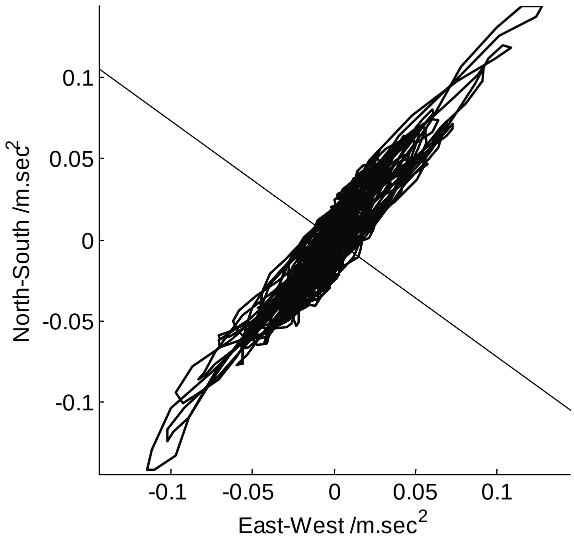

Figure 11a Acceleration values during winds registered as SSW, 39 mph (17.4m/sec)

Figure 11b Acceleration values during winds registered as WNW, 22mph (9.8m/sec) at Met station EGBB, 080131074420

at Met station EGBB, 071209224427

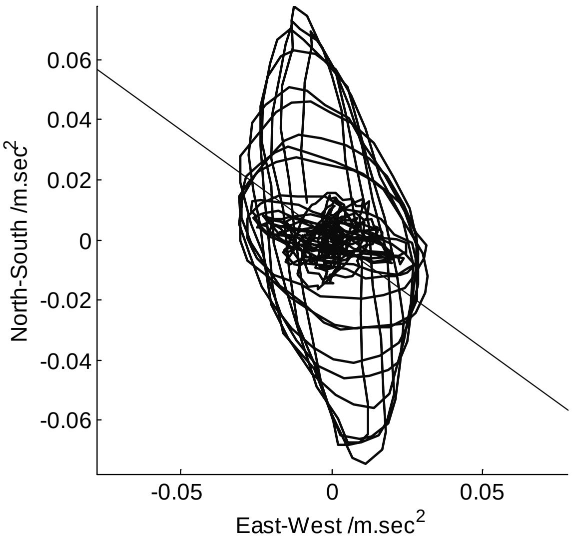

Figure 11c Acceleration values during winds registered as W, 26 mph (11.62) at Met station EGBB, 071202155622

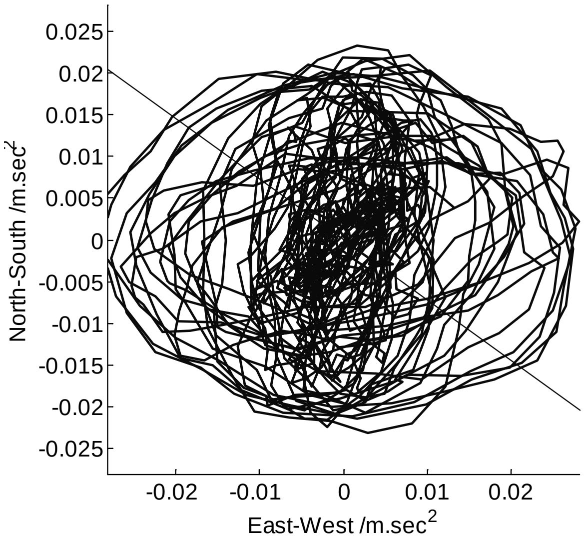

Figure 11d Acceleration values during light winds EGBB, 071117184451

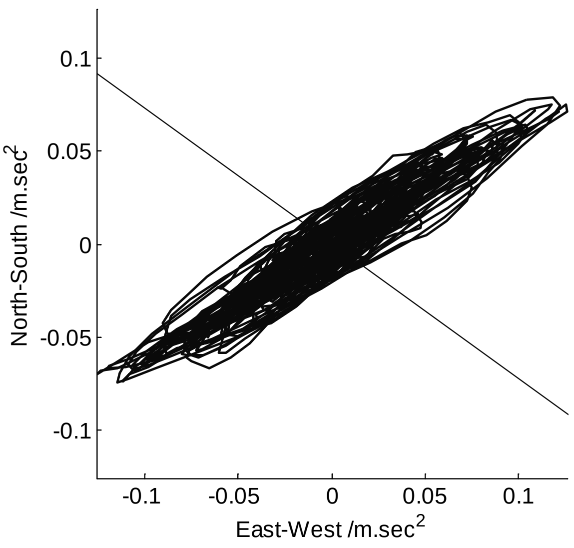

Figure 11e SSE 22-24mph (9.8-10.7m/sec), 080203170132

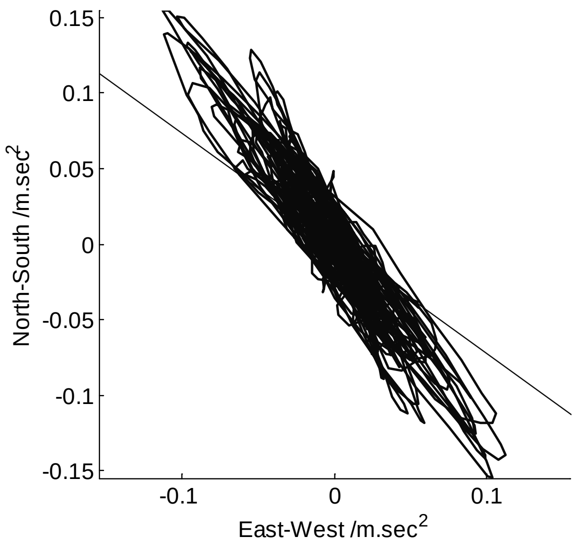

Figure 11f, 30mph (13.4m/sec) W, 080312033039

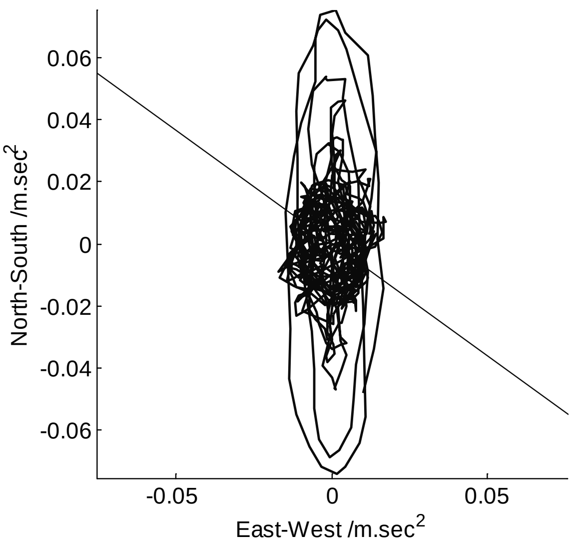

Figure 11g ENE 15mph (6.7m/sec), 071217184635

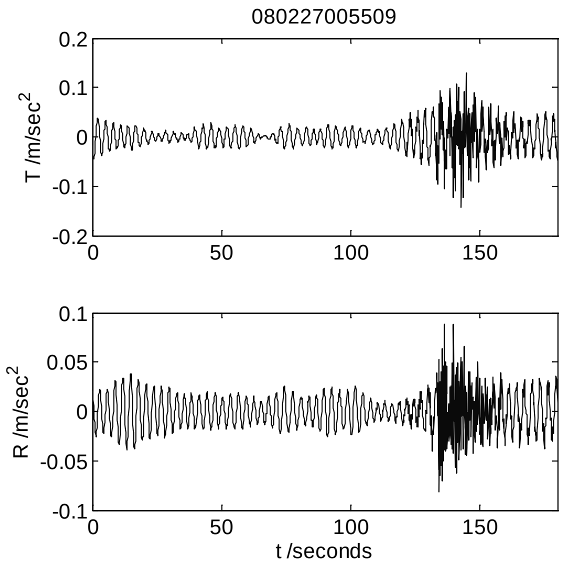

Figure 11h Response during Market Rasen earthquake, February 27 2008.

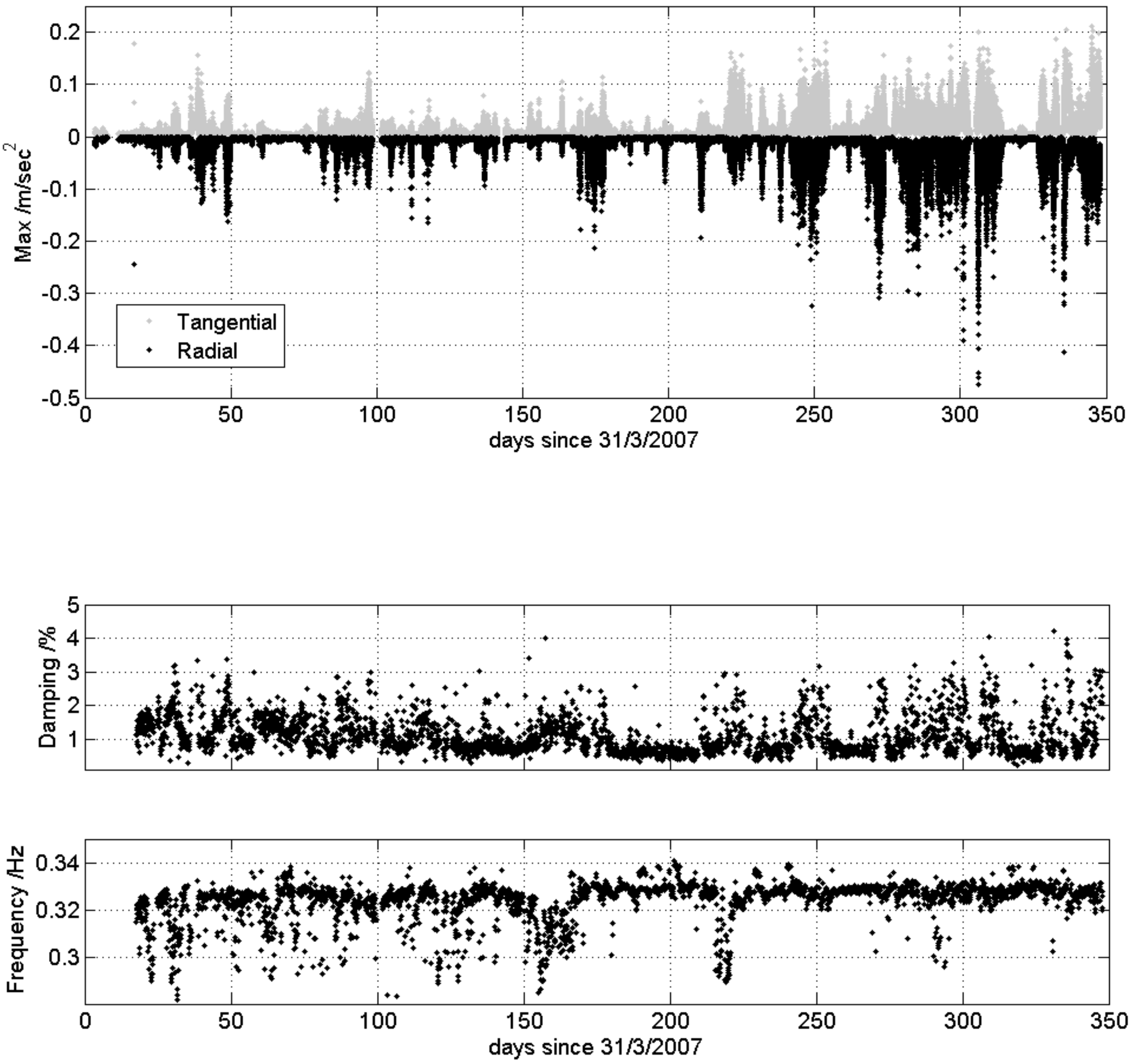

Figure 12 (upper) maximum acceleration values over 3-minute frames, (lower) damping and frequency estimates over 2-hour frames

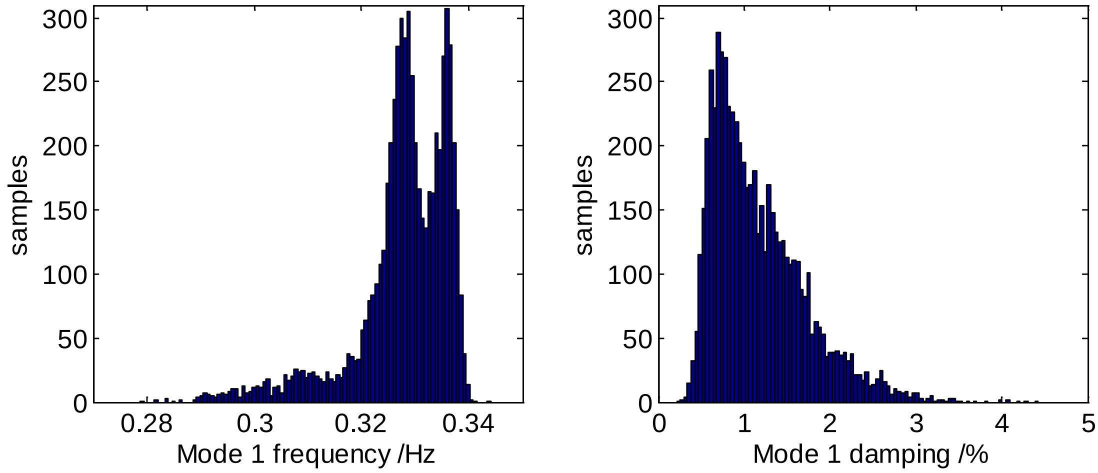

Figure 13 Distribution of first mode frequency and damping ratios until March 2008

Black and white versions of colour figures

Figure 1 Chimney at Rugeley Power station

Figure 2 New Chimney under construction

Figure 4 Accelerometer boxes, with curved and slotted plates for easy attachment

Figure 5 TMD under construction, with lower accelerometer box in position and flue openings flanking chimney

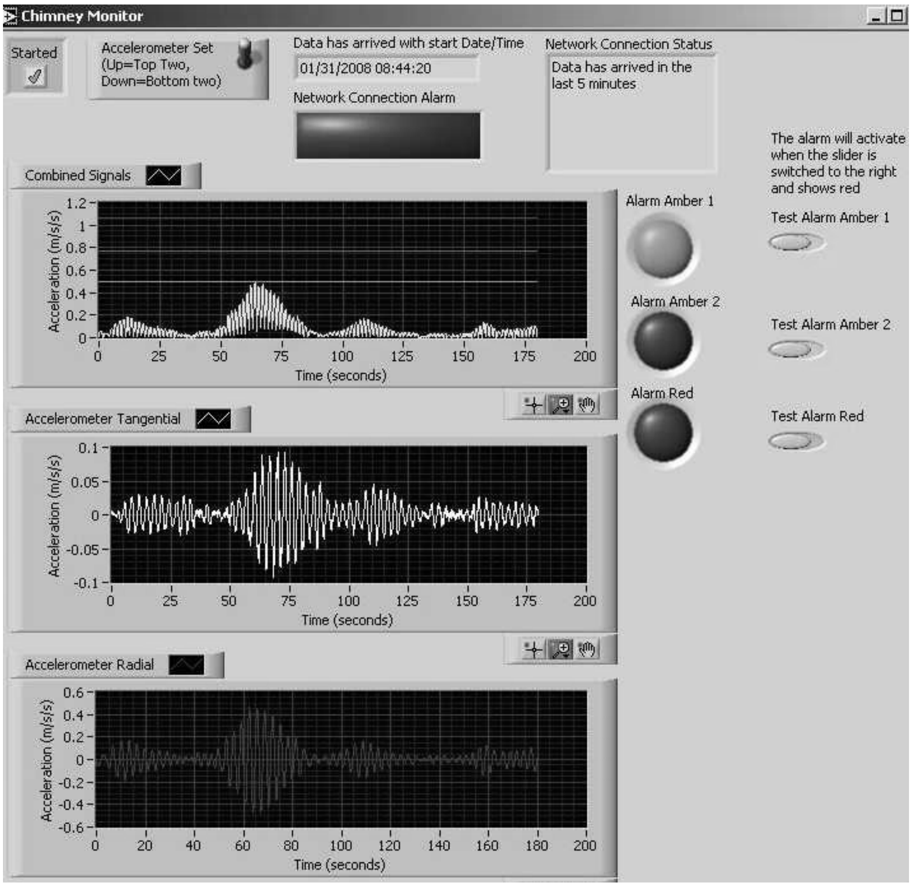

Figure 6 Monitoring system indicating alert level Amber 1, 31/01/2008

Figure 7 View from new chimney showing TMD supports, mass ring and dampers